N87-20524

# LARGE MODE RADIUS RESONATORS

Michael R Harris
Royal Signals and Radar Establishment
Malvern, Worcestershire
United Kingdom

## SUMMARY

Resonator configurations permitting operation with large mode radius while maintaining good transverse mode discrimination are considered. Stable resonators incorporating an intracavity telescope and unstable resonator geometries utilizing an output coupler with a Gaussian reflectivity profile are shown to enable large radius single mode laser operation. Results of heterodyne studies of pulsed $CO_2$ lasers with large (11mm $e^{-2}$ radius) fundamental mode sizes are presented demonstrating minimal frequency sweeping in accordance with the theory of laser-induced medium perturbations.

## INTRODUCTION

In pulsed $CO_2$ lasers both plasma effects and a laser-induced effect (LIMP) lead to frequency sweeping (1), of these, particularly for longer pulse operation, LIMP is the major offender. This chirp process exhibits an inverse 4th power dependence on beam spot size, hence a laser which has a large intracavity beam diameter can be expected to show a minimal laser-induced frequency sweep. Further advantages accrue from such a geometry; large mode volumes are obtainable from short resonators thus allowing high energy operation from compact structures, furthermore since the energy is dispersed over a large area of the mirror surface, good resistance to mirror damage should ensue. Unfortunately single mode operation from large mode radius resonators is not readily achievable; therefore, it is intended in this paper to consider possibilities for large single mode operation.

## STABLE RESONATORS

Smooth Gaussian intracavity mode profiles coupled with relative insensitivity to mirror misalignment are desirable features associated with lasers employing stable resonators.

Figure 1 shows a plot derived from the analysis of Kogelnik and Li (2) of beam spot size versus $g_1\ g_2$ where $g_1 = 1 - L/R_1$ and $g_2 = 1 - L/R_2$, L is cavity length and $R_1$ and $R_2$ are the radii of curvature of the two laser mirrors. The resonator is stable when $0 < g_1\ g_2 < 1$, and within this regime the cavity rays are confined. The form of this plot is typical of stable resonators although this is calculated for the particular case of a 40cm long cavity having one mirror with a 5m convex radius of curvature. The beam size shown is that at the concave mirror.

## Spot Size Limitations

Over the majority of the stable region spot sizes are typically less than 2mm; it is only at the two extremes where the threshold of stability is approached that the beam blows up in size. The left hand extreme, $g_1 g_2 = 0$, represents the hemispherical cavity configuration and although the beam tends to become infinitely large at the concave mirror at the other mirror the tendency is towards an infinitely small spot. Since any ray is reflected back on itself to the focus there is no mode selectivity. Of course mirror damage problems associated with the small spot will be severe.

The right hand extreme, $g_1 g_2 = 1$, represents the equivalent plane-plane resonator configuration in which beam size is only limited by mirror dimensions. But in order to ensure fundamental mode operation a small iris needs to be inserted into the cavity to aperture the beam and introduce loss to higher order modes.

So stable resonators with large spots have little or no mode selectivity, but this only applies to simple cavities - if we are allowed to introduce other optical elements then this gives a further degree of freedom.

## Telescopic Stable Resonator

Hanna et al (3) have demonstrated a Nd:YAG laser employing a stable resonator with a x4 intracavity telescope. This laser exhibits good fundamental mode operation yet produces a large beam over a portion of the cavity.

Figure 2 shows this resonator configuration applied to the $CO_2$ wavelength (4). An electron beam sustained discharge (5) is used to pump the pulsed gain module; this technique is a convenient and reliable way to operate larger cross section discharges and has the advantage that long pulse (several microseconds) operation can be assured. Since one leg of the resonator comprises a small diameter beam it is possible to hybridize the laser by the insertion of a low pressure cw gain cell, thus ensuring SLM operation as well as achieving a degree of gain switched spike suppression. The telescope is x4 and of Galilean configuration in order to avoid air breakdown problems associated with an intracavity focus. Overall cavity length is 1.75m and is invar spaced. Both the 100%R mirror and the 70%R output coupler are plane and to ensure that the cavity is an equivalent confocal resonator the telescope is slightly defocussed.

Figure 3 shows the near field beam profile of the output which has a Gaussian-like appearance, a best fit Gaussian to this profile has an $e^{-2}$ intensity radius of 11.2mm which agrees well with the theoretical prediction of 10.9mm.

Single mode operation was confirmed by examination of the cw output on a CMT detector; no beats were detected over the 0-100MHz bandwidth of the detector. The mode purity is further confirmed by the lack of beats on the power vs time waveform shown in figure 4. The gain switched spike is only partially suppressed here, presumably due to the low intracavity intensity of the cw radiation in the expanded portion of the beam within the pulsed gain region.

Shown in figure 5 is a typical beat signal between the pulsed output and a local oscillator. The output energy is 1.1J, the heterodyne signal being obtained from the scattered radiation off the joule meter surface. Measurement of peak positions

enables a frequency versus time plot to be generated and figure 6 represents on overlay of several such measurements of pulses ranging in energy between 0.64J and 1.1J. No trend in energy is observable and the plots are essentially flat indicating that LIMP is negligible. Any residual shape is most probably attributable to plasma effect.

A plot of normalized chirp coefficient against beam spot size showing the inverse 4th power dependence is depicted in figure 7. Plotted in the figure is the result with the 11.2mm beam radius shown falling close to the theoretical line of slope -4 demonstrating that the extrapolation to large spots is valid. This confirms that the technique of operating with a large intracavity mode is successful in overcoming the laser-induced chirp.

Larger magnifications than the x4 telescope used here are feasible, unfortunately the power density in the small beam leg of the resonator becomes extremely high as the mode volume and hence pulse energy is increased and ultimately mirror damage becomes a limiting factor. Clearly a configuration producing large spot sizes throughout the resonator is a necessary requirement.

## UNSTABLE RESONATORS

### Hard Mirror Unstable Resonators

In unstable resonators (6) the rays are divergent and are allowed to spread off the mirror surfaces with characteristically high losses. The leakage of radiation around the periphery of one mirror often forms the useful laser output. Unstable resonators offer a solution to the problem of filling large mode volumes but must be viewed with some reservation. Unlike stable resonators the mode properties are not well understood, the modes are not smoothly varying in intensity but are characteristically rippled, a feature which cannot be conducive to minimizing the laser-induced frequency sweep. A further problem pertinent to the realization of a fieldable laser is the tendency of these resonators to be highly alignment sensitive.

### Gaussian Mirror Resonators

Operation of a laser with an unstable resonator incorporating an output coupler with a Gaussian reflectivity profile has been demonstrated (7). This technique largely overcomes the problems associated with unstable resonators; the intracavity mode is constrained to be Gaussian and the system shows relative insensitivity to mirror misalignment.

A feature of these cavities is that although the geometric configuration is that of an unstable resonator the rays are in fact confined so that the resonators are arguably stable. This arises because the spot reflected from the Gaussian mirror is reduced in size relative to the spot incident upon it. The Gaussian beam incident upon the mirror can be expressed as

$$I_i(r) = I_{io} \exp - (2r^2/\overleftarrow{w}_1^2)$$

the mirror intensity reflectivity profile as

$$R(r) = R_o \exp - (r^2/w_{int}^2)$$

The reflected beam is the product of these two Gaussians:

$$I_i(r) = I_i(r)R(r)$$

$$= I_{io}R_o \exp - \left[(2r^2/\overleftarrow{w}_1^2) + (r^2/w_{int}^2)\right]$$

$$= I_{ro} \exp - (2r^2/\overrightarrow{w}_1^2)$$

Thus

$$\frac{1}{\overrightarrow{w}_1^2} = \frac{1}{\overleftarrow{w}_1^2} + \frac{1}{2w_{int}^2}$$

where r is radial distance; $\overrightarrow{w}_1$ and $\overleftarrow{w}_1$ are the $e^{-2}$ intensity radii of the right and left travelling beams respectively when the Gaussian mirror is at the left; and $w_{int}$ is the $e^{-1}$ reflectivity intensity radius of the Gaussian mirror (GM).

The graph shown in figure 8 plots the ratio of spot size reflected from the Gaussian mirror to the mirror Gaussian profile size as a function of $g_1g_2$. Although calculated for a 5m convex GM the plot, with only minor deviations, is general to GM resonators. In the stable region the beam radius is essentially the same as a conventional hard mirror resonator, an interpretation is that since the spot is small only the central portion of the GM is addressed over which the variation in reflectivity is small, ie the GM looks much like a conventional hard mirror. But, as the incident beam blows up in size the GM asserts itself and ultimately as the incident spot size tends to infinity the reflected spot tends to $\sqrt{2}\ w_{int}$.

In recent work at RSRE a Gaussian mirror has been incorporated in a short resonator 40cm long, this cavity length has been chosen not only for compactness but also to try to ensure SLM* operation. The e-beam sustained discharge module mentioned earlier was used again in this arrangement. The results of a scan across the GM in order to measure its reflectivity profile are shown in figure 9. Fitted to the experimental points is the best fit Gaussian which for this particular section has an $e^{-1}$ intensity radius of 9.33mm, but the profile is not perfectly circular and varies depending on scan direction between 9.1mm and 10.0mm.

Figure 10 is a plot of beam spot sizes calculated for such a 40cm long cavity having a convex 5m radius of curvature GM with an $e^{-1}$ intensity reflectivity radius ($w_{int}$) of 10mm. Along the top is indicated the radius of curvature of the hard mirror for which the specific value used was 8m concave giving beam radii in the vicinity of 10-11mm.

Reproduced in figure 11 is the near-field beam profile of the output from the laser utilizing this cavity configuration. Taking into account the uncertainty in $w_{int}$ the beam dimensions are in agreement with theory. The central dip arises from the relatively high on-axis reflectivity of the Gaussian reflectivity output coupler. Lavigne (7) have demonstrated that the propagation characteristics of a beam with such a near field profile are good, the far field profile being nearly Gaussian and free of side lobes.

---

*Single Longitudinal Mode (SLM).

A power-time waveform of the laser output is shown in Figure 12; the lack of mode beating confirms the good mode selectivity of this GM resonator. The good transverse mode discrimination is unsurprising when the weighted mean reflectivity of 40% for the fundamental (on axis) mode is compared with the $TEM_{01}$ mode value of only 20%. On faster timescales longitudinal mode beating is just discernible but again - although perhaps more surprisingly - rejection is very good the mode ratio being greater than $10^4$ for the 40cm cavity length used here.

Figure 13 shows the beat signal between the GM resonator laser output and a local oscillator. The output pulse energy is just over 1J. The beat frequency is remaining essentially constant throughout the pulse at $3.85 \pm 0.25$ MHz.

## CONCLUSIONS

Large mode radius resonators offer potential for high output energies from compact laser structures with good resistance to mirror damage as well as for minimizing LIMP. The effectiveness of such resonators in minimizing the laser-induced-frequency sweep has been demonstrated at output energies of 1J for pulses several microseconds long. The GM resonator shows much promise for large single mode operation, the intracavity mode has a Gaussian profile, transverse mode discrimination is high and the cavities are reasonably insensitive to mirror misalignment.

## REFERENCES


1. D V Willetts: Review of the Frequency Stabilization of TEA $CO_2$ Laser Oscillators, NASA/RSRE Workshop on Closed-Cycle, Frequency-Stable $CO_2$ Laser Technology, NASA CP-2456, 1987.

2. H Kogelnik and T Li: Laser Beams and Resonators Appl Opt 5 (1966) pp 1550-67.

3. D C Hanna, C G Sawyers, M A Yuratich: Telescopic Resonators for Large-Volume $TEM_{oo}$-mode Operation, Optical and Quantum Electronics 13 (1981) pp 493-507.

4. D V Willetts and M R Harris: Attainment of Frequency Stable High-Energy Operation of a $CO_2$ TEA Laser by Use of a Telescopic Resonator, IEEE J Q.E. 21 No 3 (1985) pp 188-191.

5. A Crocker, H Foster, H M Lamberton and J H Holliday: Pulsed Atmospheric Pressure Carbon Dioxide Laser Initiated by a Cold Cathode Glow-Discharge Electron Gun, Electron Lett 8 No 18 (1972) PP 460-461.

6. A E Siegmann: Unstable Optical Resonators, Applied Optics 13 No 2 (1974) pp 353-367.

7. N McCarthy and P Lavigne: Large Size Gaussian Mode in Unstable Resonators Using Gaussian mirrors, Optics Letters 10 No 11 (1985) pp 553-555.

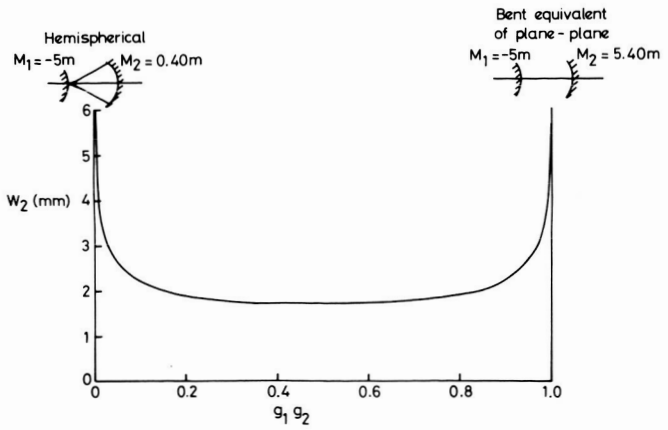


STABLE RESONATOR MODE RADIUS VS $g_1 g_2$ ($\lambda = 10.6\mu$, $R_1 = -5.0m$, $L = 0.40m$)

Figure 1.

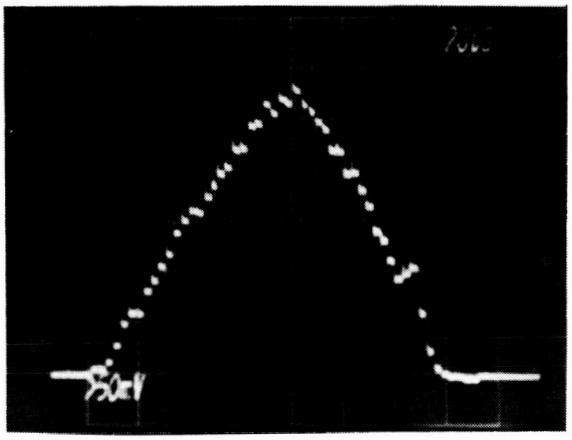

Near-field section of telescopic resonator laser output; pitch of elements = 0.5mm

Figure 3.

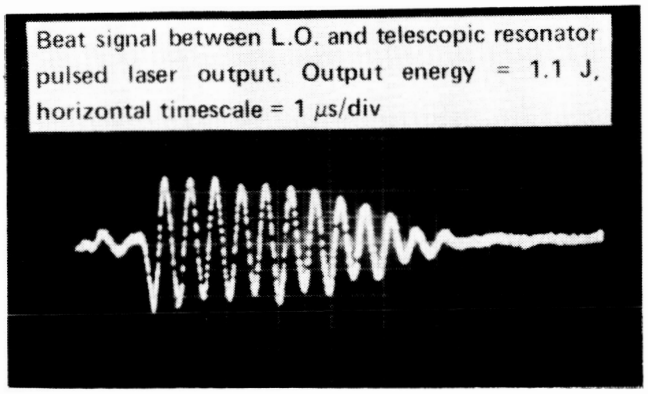


Figure 5.



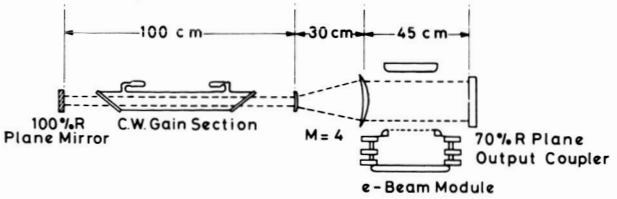


Hybrid e-beam sustained $CO_2$ laser with telescopic resonator

Figure 2.

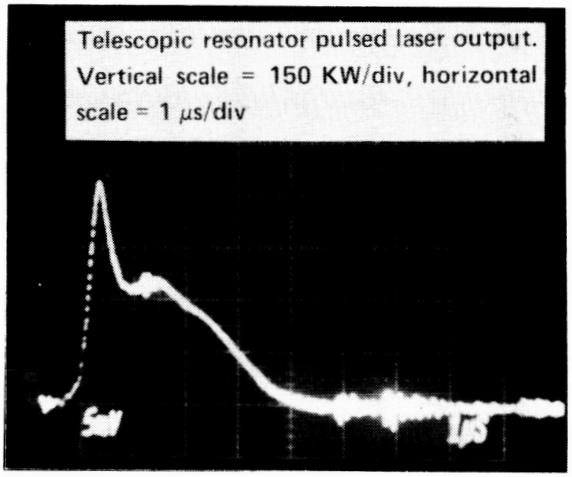


Figure 4.

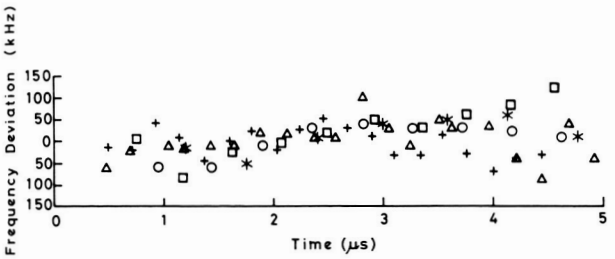


Telescopic resonator laser; temporal variation from mean of beat frequency for the following output energies
□ = 0.64 J; + = 0.70 J; * = 0.85 J;
0 = 1.00 J; Δ = 1.07 J.

Figure 6.

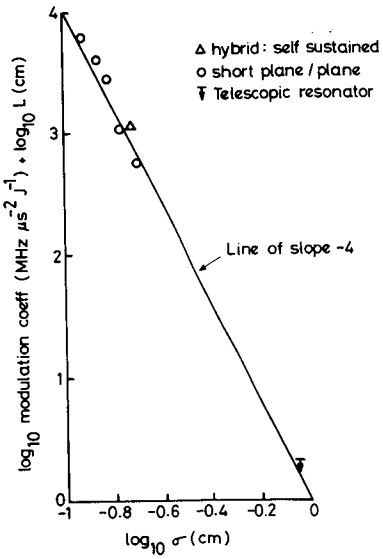


NORMALISED MODULATION COEFFICIENT VERSUS BEAM RADIUS SHOWING PREDICTED INVERSE 4th POWER DEPENDENCE

Figure 7.

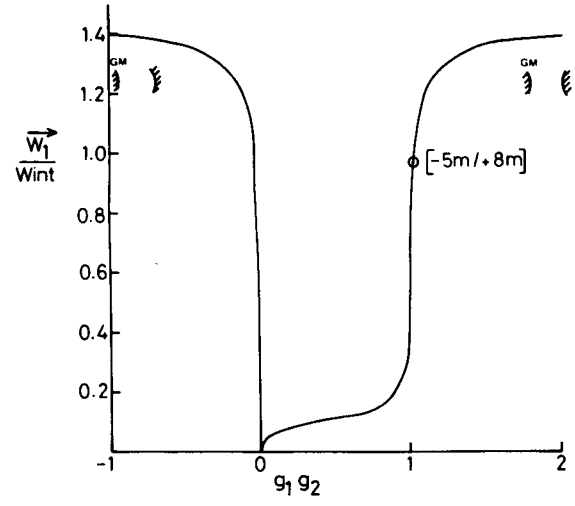


GAUSSIAN RESONATORS: NORMALISED SPOTSIZE REFLECTED FROM GAUSSIAN MIRROR

Figure 8.

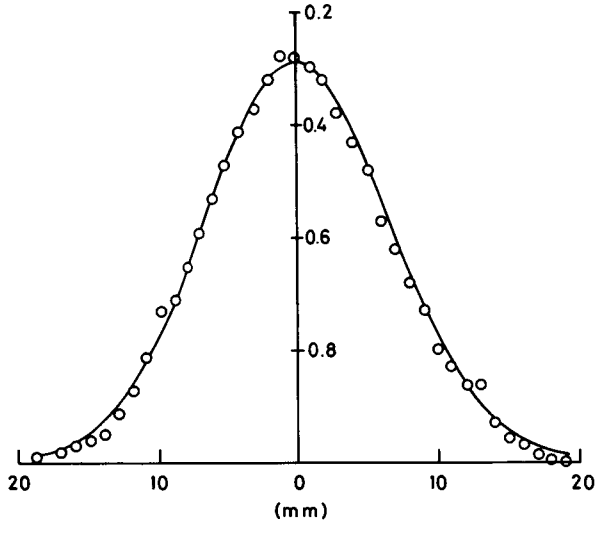


RADIAL TRANSMISSION PROFILE OF GAUSSIAN MIRROR
(fit to curve w = 9.33 mm)

Figure 9.

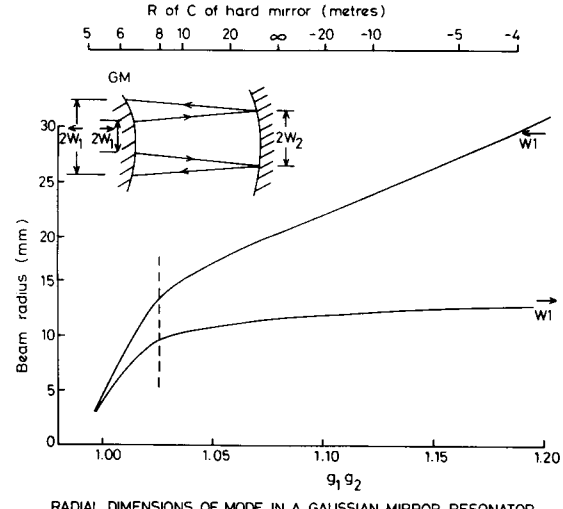


RADIAL DIMENSIONS OF MODE IN A GAUSSIAN MIRROR RESONATOR
(R OF C = 5m VEX, WINT = 10 mm)

Figure 10.

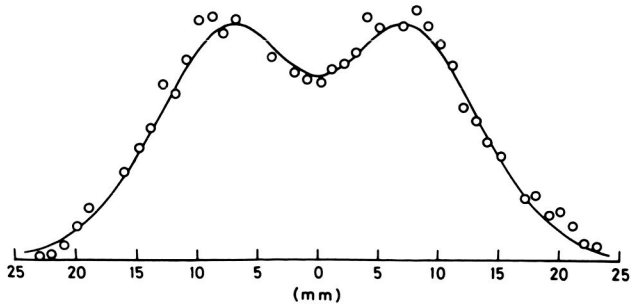


NEAR FIELD (d = 1.2 m) TRANSVERSE PROFILE OF GAUSSIAN MIRROR RESONATOR

Solid line calculated assuming w = 15.9 mm, $w_{int}$ = 11.5 mm, $R_{max}$ = 0.74

Figure 11.

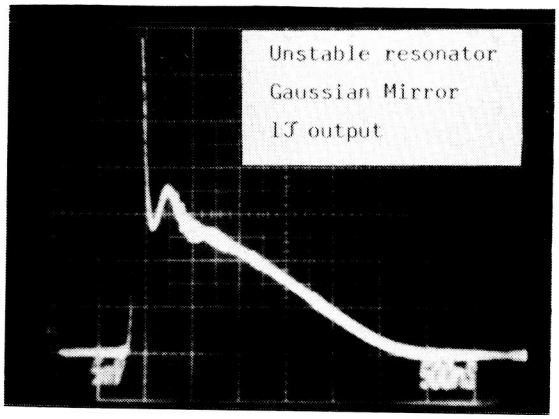


Figure 12.

Beat signal between L.O. and pulsed laser with Gaussian Resonator. Output energy = 1.1 J, horizontal time scale = 1 μs/div

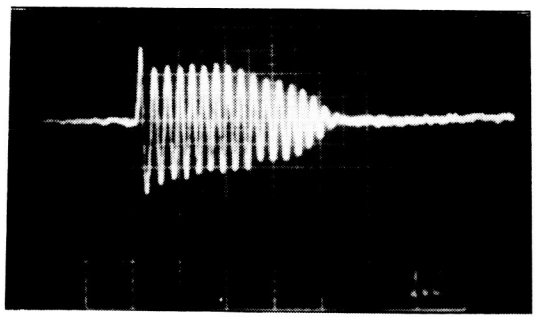

Figure 13.